Edinburgh Research Explorer

Adsorption and self-assembly of linear polymers on surfaces: a computer simulation study

Adsorption and self-assembly of linear polymers on surfaces: a computer simulation study**

A. Chremos,[1] E. Glynos,[2,†] V. Koutsos[2] and P.J. Camp[1,*]

[1]EaStCHEM, School of Chemistry, Joseph Black Building, University of Edinburgh, West Mains Road, Edinburgh, EH9 3JJ, UK.

[2]Institute for Materials and Processes, School of Engineering and Electronics, and Centre for Materials Science and Engineering, The University of Edinburgh, Mayfield Road, Edinburgh, EH9 3JL, UK.

[†]Present address: Department of Materials Science and Engineering, University of Michigan, Ann Arbor, MI 48109-2136, USA.

[*]Corresponding author; e-mail: philip.camp@ed.ac.uk

Graphical abstract:
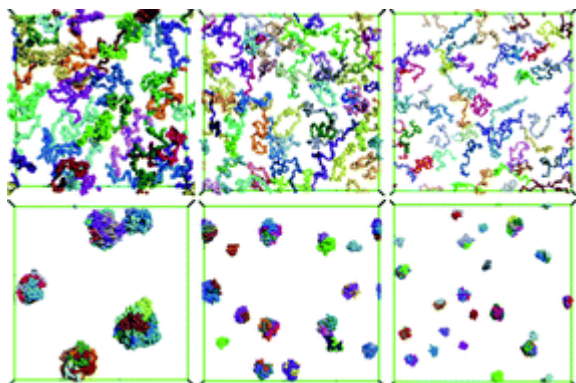
Summary:
Computer simulations are used to gain insight on polymer adsorption and self assembly on smooth surfaces, as studied in recent atomic force microscopy experiments.

Abstract

The adsorption and self-assembly of linear polymers on smooth surfaces are studied using coarse-grained, bead-spring molecular models and Langevin dynamics computer simulations. The aim is to gain insight on atomic-force microscopy images of polymer films on mica surfaces, adsorbed from dilute solution following a good solvent-to-bad solvent quenching procedure. Under certain experimental conditions, a bimodal cluster distribution is observed. It is demonstrated that this type of distribution can be reproduced in the simulations, and rationalized on the basis of the polymer structures prior to the quench, i.e., while in good-solvent conditions. Other types of cluster distribution are described and explained. Measurements of the fraction of monomers bound to the surface, the film height, and the radius of gyration of an adsorbed polymer chain are also presented, and the trends in these properties are rationalized. In addition to providing insight on experimental observations, the simulation results support a number of predicted scaling laws such as the decay of the monomer density as a function of distance from the surface, and scaling of the film height with the strength of the polymer -surface interactions.

1. Introduction

Polymers near to, or adsorbed on, surfaces exhibit useful and interesting properties. Adsorbed polymers find application in colloid stabilization,[1,2] nanoscale surface patterning ,[3] friction modification,[4,5] DNA microarrays[6] and adhesion.[7] Polymers can be attached to appropriate surfaces either through chemisorption/grafting (*i.e.*, anchoring by chemical bonds) or by physisorption (*i.e.*, chain attachment by van der Waals interactions). For a weakly adsorbing surface the physisorption and resulting conformational relaxation of the chain is driven by the competition between the entropic repulsion due to the loss of conformational freedom and the drop in energy from binding monomers to the substrate. Earlier investigations have focused on thin-film polymer blends,[8–10] block copolymer micelles adsorbed on surfaces,[11–13] end-grafted polymers chemisorbed on surfaces,[14–16] and several other complex systems. The simple case of homopolymer chains physisorbed on a substrate has been studied with simulations of free[17–23] and tethered chains,[24–26] and through theoretical approaches;[27–29] experimental studies, however, are scarce.

In recent work by our groups , we studied the physisorption and self-assembly of star[30] and linear[31] polymers on smooth surfaces using atomic-force microscopy (AFM). In a typical experiment, a polymer solution was prepared in a good solvent at concentrations below the critical overlap volume fraction ($\phi*$), resulting in well-separated chains in solution and hence precluding any strong degree of structural ordering within the polymer component. Polymer (sub-)monolayers were formed by exposing a smooth surface (such as highly ordered pyrolytic graphite or mica) to the polymer

solution. The surface was then placed in a good solvent bath for several hours and extensively rinsed with good solvent to remove any non-adsorbed polymer . Finally, the samples were dried gently under a stream of nitrogen and subsequently imaged in air by AFM in tapping mode to investigate the resulting structures from this good solvent-to-bad solvent 'quench'. Depending on the polymer molecular weight, architecture, and concentration, very different surface structures can be obtained. For the case of star polymers it was found that the functionality (number of arms) and concentration of star polymers controls a crossover between 'polymer ' and 'soft-colloid' regimes, being distinguished by characteristic cluster topologies, sizes, and surface coverages.[30] Using the same experimental procedure, we have now studied the adsorption of linear polybutadiene (PB) on to mica from toluene. A report of this investigation is in preparation,[31] but for the purposes of the current work, we present one key experimental observation on which we will aim to gain insight using computer simulations. In Fig. 1(a) we present an AFM image of a freshly cleaved mica surface exposed for 30 minutes to a toluene PB solution (molecular weight 78.8 kg mol^{-1}) leading to a surface coverage of 7.75×10^{-2} mg m^{-2}. This image shows two distinct types of cluster . In Fig. 1(b) we show the corresponding bimodal cluster -height distribution, with most probable heights of approximately 1 nm and 6 nm. In this work we aim to reproduce, and gain insight on, the development of bimodal cluster distributions using Langevin dynamics simulations of coarse-grained 'bead-spring' models of linear polymers .
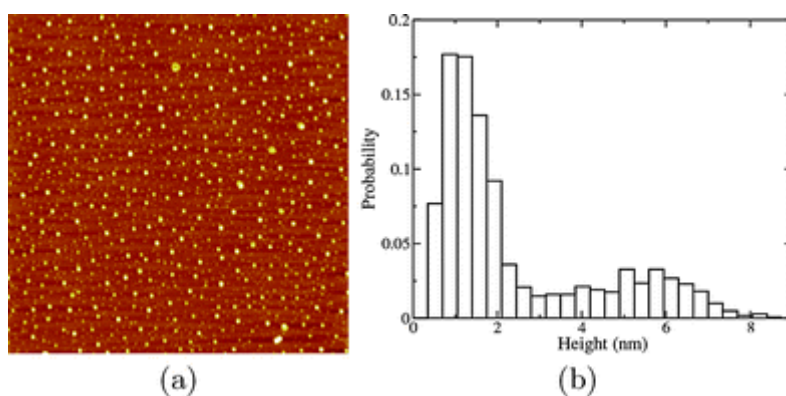
Figure 1. (a) AFM image of linear polybutadiene (molecular mass 78.8 kg mol^{-1}) adsorbed on mica from toluene at a surface concentration of 7.75×10^{-2} mg m^{-2}. The image size is 6×6 μm^2. (b) Cluster -height distribution corresponding to the AFM image in (a).

In the experimental quenching procedure described above, the microscopic structures of the polymer solutions in contact with surfaces prior to quenching must control the nature of polymer adsorption. Hence, the behaviour of polymers in good-solvent conditions and near a surface is of considerable

interest. In the past, adsorption and depletion-layer effects have been the subjects of many experimental, theoretical, and computer-simulation studies. Of particular relevance to the current work is the seminal study by de Gennes focused on the monomer volume-fraction profile $\phi(z)$ as a function of the perpendicular distance from the surface z.[32] De Gennes considered a semidilute solution of chains in contact with a weakly attracting wall, with the wall-monomer interaction of a range comparable to the monomer size a. In the semidilute regime, the polymer volume fraction in solution $\phi_b > \phi*$, meaning that there are overlapping chains. Near the wall, chains are physisorbed through a small number of monomers, leading to the formation of loops with characteristic dimension $D > a$. Well away from the wall, the characteristic length scale is the bulk correlation length $\xi_b \sim \phi_b^{-3/4}$,[27] which in the semidilute regime is comparable to the polymer radius of gyration R_G in bulk solution. Three regimes of z can be identified: the *proximal* regime $z \simeq a < D$ where $\phi(z)$ is dictated by the short-range interactions with the wall; the *central* regime $D < z < \xi_b$ in which 'no other length enters in the problem'[32] meaning that if $\xi[\phi(z)] \simeq z$ and $\xi(z) \sim \phi(z)^{-3/4}$ then $\phi(z) \sim z^{-4/3}$; and the *distal* regime $z > \xi_b$ where $[\phi(z) - \phi_b]/\phi_b \sim \exp(-z/\xi_b)$. The structure in the central regime is 'self-similar' or 'scale-free', because there is no characteristic length scale (unlike in the proximal or distal regimes, which are characterized by a and ξ_b, respectively). The existence of a self-similar structure characterized by an exponent of $-4/3$ has been confirmed experimentally by neutron scattering [33] and by neutron reflectivity .[34–36] Results from Monte Carlo simulations of lattice polymer models are also consistent with this behaviour.[37–39] An incidental result of the current work is a demonstration that a coarse-grained, off-lattice polymer model can reproduce this self-similar structure, and with the correct exponent.

In this paper we report a simulation study of adsorbed linear-polymer films. We use Langevin dynamics simulations of coarse-grained 'bead-spring' models to gain insight on the results from polymer adsorption experiments. The outline of the study is as follows. Firstly, we study the properties of isolated adsorbed polymers (vanishing surface coverage). This situation has been considered many times before (see, *e.g.*, Ref. 23), but for the purposes of comparison with the case of finite surface coverage, we reconsider specific single-molecule structural properties for the particular coarse-grained models being employed. Next, we deal with many polymers on a surface under good solvent conditions, corresponding to the prelude of the bad-solvent quench in experiments. Of particular interest are simulation measurements of $\phi(z)$ and the comparison with de Gennes' theoretical predictions. Finally, we simulate the good solvent-to-bad solvent quench, and its effects on the structure of the polymerfilm. Specifically, we identify under what conditions a bimodal cluster distribution (such as those seen in experiments—Fig. 1) should be expected. The paper is organized as follows. Section II contains details of the coarse-grained polymer model, and the simulation methods. Results for isolated polymers and many polymers are presented in Section III. Section IV concludes the paper.

Simulation model and methods

Linear polymers are modelled as chains of N coarse-grained 'beads' connected by 'springs'. The physical motivation for such a model stems from the fact that correlations between monomers die off beyond a characteristic length, called the Kuhn length b. Hence, if a number of contiguous monomers are rendered by a single bead of dimension b, then the scaling properties of the chain on length scales larger than b will be left invariant.[27,40,41] Such bead-spring models of linear and star polymers were first introduced and employed in simulations by Grest and co-workers.[42–45] In this work, N beads of equal mass m are connected to form a chain using a non-linear finitely extensible (FENE) potential between neighbouring beads, given by

$$V_{\text{FENE}}(r) = -\frac{1}{2}kR_0^2 \ln\left(1 - \frac{r^2}{R_0^2}\right)$$

(1)

Here r is the bead-bead separation, R_0 is the maximum possible (bonded) bead-bead separation, and k is a spring constant. In this study we use parameters from earlier work,[43] namely $R_0 = 3\sigma/2$ and $k = 30\varepsilon/\sigma^2$; ε and σ are the energy and range parameters, respectively, for the non-bonded interactions to be defined next.

The non-bonded interactions operate between all pairs of beads, and are derived from a composite potential devised by Steinhauser.[46] The potential is a combination of three terms. First we write the purely repulsive Weeks-Chandler-Andersen (WCA) potential,[47] which is a Lennard-Jones potential cut and shifted at the position of the minimum, $r_{\text{min}} = 2^{1/6}\sigma$:

$$V_{\text{WCA}}(r) = \begin{cases} 4\varepsilon\left[\left(\frac{\sigma}{r}\right)^{12} - \left(\frac{\sigma}{r}\right)^6\right] + \varepsilon & r \leq r_{\text{min}} \\ 0 & r > r_{\text{min}} \end{cases}$$

(2)

To represent the attractive interactions, the WCA potential is shifted back down in the range $0 \leq r \leq r_{\text{min}}$ by a square-well (SW) potential

$$V_{\text{SW}}(r) \begin{cases} -\lambda\varepsilon & 0 < r \leq r_{\text{min}} \\ 0 & r > r_{\text{min}} \end{cases}$$

(3)

where λ reflects the solvent quality (to be discussed below). To interpolate the potential smoothly between $-\lambda\varepsilon$ at $r = r_{\text{min}}$ and 0 at a cut-off distance $r_{\text{cut}} > r_{\text{min}}$, we add the term

$$V_{cos}(r) = \begin{cases} \dfrac{1}{2}\lambda\varepsilon\Big[\cos(\alpha r^2 + \beta) - 1\Big] & r_{min} < r \le r_{cut} \\ 0 & r > r_{cut} \end{cases} \qquad (4)$$

α and β satisfy the conditions $\alpha r_{min}^2 + \beta = \pi$ and $\alpha r_{cut}^2 + \beta = 2\pi$. The cosine form of the potential also means that $dV_{cos}/dr = 0$ at $r = r_{cut}$. Following earlier work,[46] we choose $r_{cut} = 3\sigma/2$, for which the appropriate parameters are

$$\alpha = \frac{4\pi}{9 - 4\sqrt[3]{2}} = 3.173\ 072\ 868 \qquad (5)$$

$$\beta = 2\pi - \frac{9}{4}\alpha = -0.856\ 228\ 645 \qquad (6)$$

The final, non-bonded potential is $V(r) = V_{WCA}(r) + V_{SW}(r) + V_{cos}(r)$, and is sketched in Fig. 2. The parameter λ controls the depth of the potential well at $r = r_{min}$, and provides a convenient measure of the solvent quality. In a good solvent , the effective bead-bead interactions are purely repulsive; this corresponds to $\lambda = 0$. In a bad solvent , the bead-bead interactions are attractive, and this behaviour can be modelled with $\lambda = 1$; this corresponds to an attractive well of depth ε which sets the molecular energy scale. θ-solvent conditions—under which the chain statistics are very similar to those for an ideal (non-interacting) chain—are reproduced by $\lambda = 0.646$.[46]
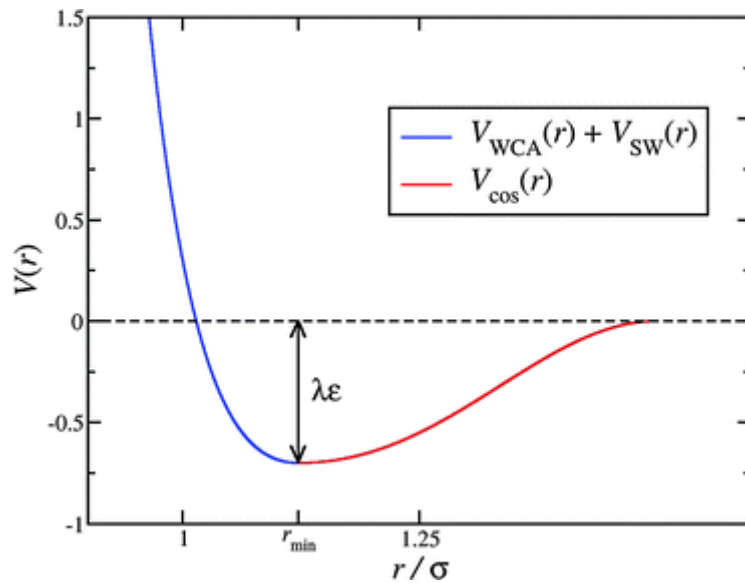

Figure 2. The non-bonded, bead-bead interaction potential $V(r)$ with $\lambda = 0.7$, showing the contributions from $V_{WCA}(r) + V_{SW}(r)$ (blue) and $V_{cos}(r)$ (red).

For simulations involving a surface, an additional effective bead-surface potential is used,[45] based on integrating the Lennard-Jones interactions arising from a homogeneous distribution of sites within the surface. The potential is

$$V_s(z) = \frac{2\pi\varepsilon_s}{3}\left[\frac{2}{15}\left(\frac{\sigma}{z}\right)^9 - \left(\frac{\sigma}{z}\right)^3\right]$$

(7)

where z is the perpendicular distance of the bead from the surface, and ε_s controls the strength of the bead-surface attraction. In our simulations we define ε_s in terms of the basic energy parameter ε by defining the dimensionless ratio $\varepsilon^*_s = \varepsilon_s/\varepsilon$. In practice, we concentrated on the values in the range $0.4 \leq \varepsilon^*_s \leq 1$.

For simulating the bead-spring polymer chains, we used Langevin dynamics in which the system is coupled to a heat bath, corresponding physically to solvent . In addition to the conservative forces arising from the interaction potentials described above, each bead will feel random and frictional forces mimicking the solvent surrounding the bead. Thus the equations of motion for bead i are given by

$$m\frac{d^2r_i}{dt^2} = -\nabla_{r_i}V - m\Gamma\frac{dr_i}{dt} + W_i(t)$$

(8)

where Γ is the friction coefficient, $W_i(t)$ describes the Brownian forces of the solvent acting on the bead, and $V = \sum_{i<j}V_{ij}$ is the total interaction potential. $W_i(t)$ is represented by Gaussian white noise satisfying the fluctuation-dissipation theorem[48]

$$\langle W_i(t)\cdot W_j(t')\rangle = 6k_BTm\Gamma\delta_{ij}\delta(t-t')$$

(9)

Simulations were performed in an $L \times L \times H$ cuboidal box with periodic boundary conditions in all three directions and the minimum-image convention applied. The box dimension in the z direction was set to a large, but finite, value of $H = 200\sigma$, and the surface was represented by a structureless, $L \times L \times l$ solid slab with a thickness l no less than the maximum range of interaction between beads. To control the surface bead density, L took on values of 80σ through to 180σ, which were always large enough for polymers in their natural conformations to avoid interacting with their own periodic images. The simulation conditions mean that the polymers are at finite density within the simulation cell , and so there is an equilibrium state where the polymers are adsorbed. In principle, the polymers could adsorb on either face of the slab, but they cannot interact with each other because l is larger than the interaction range, and H is much larger than typical polymer dimensions (as measured by the radius of gyration, R_G); hence, the two surfaces are essentially isolated from one another. In practice, initial configurations were prepared by placing the polymers on one face of the slab, and all

subsequent measurements were made for that one surface. Simulated properties are reported here in reduced units defined in terms of m, ε, and σ. The equations of motion were integrated using the velocity-Verlet algorithm with a time-step $\delta t = 0.007\tau$, where $\tau = \sqrt{m\sigma^2/\varepsilon}$ is the basic unit of time. In all cases, the reduced temperature $k_B T/\varepsilon = 1$, and the reduced friction coefficient $\Gamma\tau = 1$.

3. Results

We have studied three different situations using Langevin dynamics simulations: (i) the behaviour of isolated polymers on surfaces with various solvent qualities (with $0 \leq \lambda \leq 1$); (ii) the behaviour of many polymers on surfaces in good-solvent conditions (with $\lambda = 0$), corresponding to the experimental situation before the good solvent-to-bad solvent quench; and (iii) many polymers in bad solvent conditions (with $\lambda = 1$) corresponding to the post-quench situation probed in AFM experiments. We have studied three different chain lengths ($N = 50$, 100, and 200 beads), a range of different surface-energy parameters $\varepsilon^*_s = \varepsilon_s/\varepsilon$, and in the many polymer cases, a variety of surface coverages (to be defined in Section 3.B). The number of beads in each of the longest chains is of the same order of magnitude as the number of Kuhn segments in the smallest chains studied in experiments. Such coarse-grained, bead-spring models are known to reproduce faithfully the semi-quantitative properties of polymers , and so despite the small lengths of our chains, we anticipate that the various trends seen in our results will be of relevance to experiments on ultra-thin polymer films after a sudden change in the solvent quality. Our choices for ε^*_s are based on achieving a suitable degree of surface adsorption. We have not attempted the difficult problem of determining this effective interaction parameter from first principles; this would involve using atomistic representations of the surface, polymer , and solvent in order to determine the direct and solvent -mediated forces acting between the polymer and surface.

A. Isolated polymer

The average conformation of a polymer in dilute solution is well understood, and has an isotropic globular shape defined by a radius of gyration R_G, which scales with the number of monomer units N like $R_G \sim N^\nu$ where ν is the characteristic Flory exponent equal to 1/3 in a bad solvent , 1/2 in a θ-solvent, and 3/5 in a good solvent .[27] In the proximity of a surface, the number of available polymer conformations is reduced, leading to a decrease in entropy. Adsorption occurs when the surface-energy parameter ε_s exceeds a certain critical value, ε^c_s, signalling that the energetic contribution to the free-energy from polymer -surface interactions becomes significant.[27,49] The accompanying change in

polymer conformation can be interpreted as the order parameter for a type of second-order phase transition at $\varepsilon_s = \varepsilon_s^c$.[27,49] It is useful to define the dimensionless variable κ

$$\kappa = (\varepsilon_s - \varepsilon_s^c)/\varepsilon_s^c \qquad (10)$$

which measures the relative distance from the critical point. We also define the scaling variable y,

$$y = \kappa N^\phi \qquad (11)$$

where ϕ is a crossover exponent; this variable appears in the scaling analysis of polymer adsorption.[32,28] Through scaling theory, one can identify four regimes of adsorption depending on the values of y and κ. (a) For a repulsive wall, $y < 0$, the chain trivially remains away from the surface. (b) Near the critical point, $y \simeq 0$, the chain is equally likely to be found at the surface as it is in the solution. (c) When $y \gg 1$ with N large and κ small, adsorption is nonetheless favoured because the sum of the interactions of the individual beads with the surface outweighs the entropic penalty of the chain being near the wall. This situation is called the weak coupling limit.[32] (d) For $\kappa > 1$ the monomers are strongly attracted to the surface and the chain lies flat. This is called the strong coupling limit.[32] Cases (a)–(c) have been studied extensively in simulations of the particular situation where each chain is tethered to the surface by one end;[25,26] case (d) has been studied in simulations of free chains.[21–23] Earlier simulations using the same type of bead-surface potential as in eqn (7) suggest that, in reduced units, the critical surface-energy parameter $\varepsilon_s^c/\varepsilon \sim 0.1$.[26] The values of ε_s^* used in the current simulations (reported below) correspond to the strong coupling regime.

All isolated-polymer simulations began by placing a linear chain in good-solvent conditions ($\lambda = 0$) close enough to the surface for adsorption to occur. Once the chain had adsorbed, the solvent quality was adjusted by changing λ to the desired value. The molecule was equilibrated for around $10^6 \delta t$, and then properties were measured over a production run of $5 \times 10^6 \delta t$. Fig. 3(a) and (b) shows the probability density $p(z)$ of finding beads at a perpendicular distance z from the surface, from simulations of isolated polymers consisting of $N = 100$ beads, with various values of ε_s^* and λ. (The density profiles are reported in this form—normalized so that $\int_0^\infty p(z)\mathrm{d}z = 1$—to aid comparison with later results for many polymers at finite densities.) In all cases there is either a local minimum or a point of inflection in $p(z)$ at $z \simeq 1.2\sigma$, and the position of these features was taken as a distance-based criterion for assessing whether a particular bead is 'bound' to the surface or not. Note that from eqn (7) the minimum bead-surface potential energy is located at $z/\sigma = \sqrt[6]{2/5} \simeq 0.86$; this distance corresponds to the positions of the primary peaks in $p(z)$.
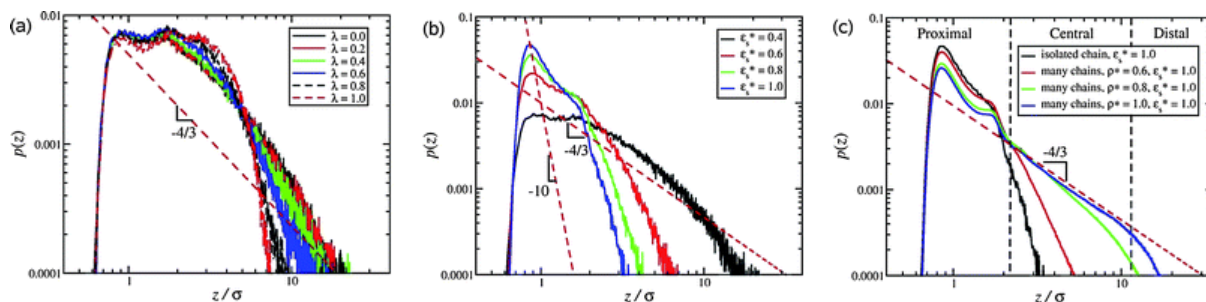
Figure 3. The probability distribution $p(z)$ of finding a bead at a perpendicular distance z from the surface. All results are for chains with $N = 100$ beads. (a) Isolated chain with $\varepsilon^*_s = 0.4$ and $0 \leq \lambda \leq 1$. (b) Isolated chain with $\lambda = 0$ (good solvent) and $0.4 \leq \varepsilon^*_s \leq 1.0$. (c) Isolated chain compared to many chains (with densities $\rho^* = 0.6$, 0.8, and 1.0), all with $\lambda = 0$ (good solvent) and $\varepsilon^*_s = 1.0$. Approximate ranges of the proximal, central and distal regimes for the system with $\rho^* = 1.0$ are indicated.

In Fig. 4 we show the average bound fraction $\langle \Phi_a \rangle$ and the average maximum height $\langle h \rangle$ as functions of λ for different chain lengths and surface-energy parameters ε^*_s. With $N = 50$, no apparently stable adsorption occurs for $\varepsilon^*_s < 0.6$, while for longer chains with $N = 100$ and 200, adsorption occurs when $\varepsilon^*_s \geq 0.4$. That is because for $\varepsilon^*_s = 0.4$ we are close to the weak coupling regime, meaning that the individual bead-surface interactions are not sufficient to keep each of them on the surface. The bound fraction $\langle \Phi_a \rangle$ is the fraction of beads within interaction range of the surface defined using the distance-based criterion $z \leq 1.2\sigma$. For all ε^*_s, $\langle \Phi_a \rangle$ remain insensitive to N. This is in agreement with theory and simulations, since for $\kappa > 1$ the bound fraction scales like $\Phi_a \sim N^0$.[50] It also remains insensitive to solvent quality. There is though only a weak monotonic decrease with increasing λ; this is due to the polymers bunching up to optimize the attractive bead-bead interactions, at the cost of bead-surface contacts. Unsurprisingly, for a given λ, increasing ε^*_s leads to a greater bound fraction.
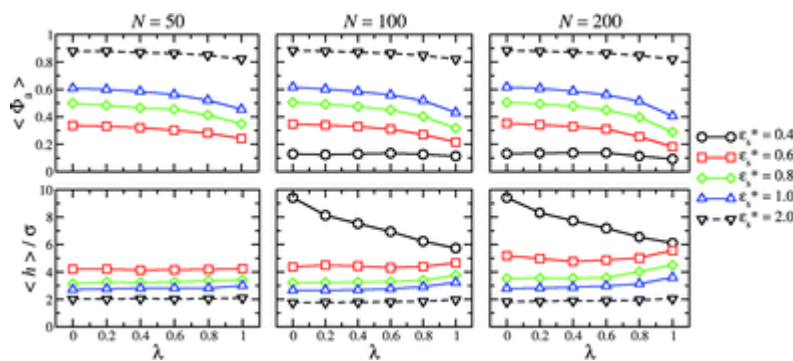
← ***Figure 4.*** The bound fraction $\langle \Phi_a \rangle$ (top) and the average maximum height $\langle h \rangle$ (bottom) against solvent quality λ for isolated linear chains with, from left to right, $N = 50$, 100, and 200 beads, and with different surface-interaction parameters ε^*_s.

In general, the average maximum height $\langle h \rangle$ for all systems with $\varepsilon^*_s \geq 0.6$ shows a very weak dependence on λ, there being only a slight hint of an increase as the bad-solvent conditions ($\lambda = 1$) are approached; this is due to the 'bunching up' of the beads, to take advantage of their mutual attractive interactions. But on the whole, the strong bead-surface interactions keep the polymers quite flat on the surface, with small, short-lived 'loops' and 'tails' appearing as beads lift off the surface as a result of thermal fluctuations.

Different behaviour is observed in those systems with $N = 100$ and 200 beads, and $\varepsilon^*_s = 0.4$, in which $\langle h \rangle$ clearly decreases with increasing λ. This, again, is due to the 'bunching up' of the polymer chain, much like an accordion being compressed. The difference here, though, is that with such a weak bead-surface interaction parameter, the polymers possess only a small number of contacts with the surface, leading to the formation of large, long-lived 'loops' and 'tails' oriented perpendicular to the surface. When λ is increased, the loops and tails contract, leading to a reduction in the height of the polymer ; but with a weak bead-surface interaction, this process occurs without the loops flattening out and forming new contacts with the surface.

B. Many polymers —good solvent

Polymers in good solvent experience purely repulsive mutual interactions. Appropriate simulations with $\lambda = 0$ were initiated by preparing configurations with many 'curled up' polymers on a surface, and equilibrating for around $10^6 \delta t$. For chains of $N = 50$, 100, and 200 beads, we initially placed 200, 100, and 50 chains on the surface, respectively, leading to the same total number of beads in each case. Following equilibration, we performed a production run of $2.5 \times 10^6 \delta t$. The adsorption is measured by the equilibrium surface bead density, defined in terms of the number of beads N_{ads} belonging to those chains with at least one bead-surface contact, defined using the distance-based criterion $z \leq 1.2\sigma$. Note that N_{ads} is, in general, greater than the number of beads actually bound to the surface. The reduced surface bead density is $\rho^* = N_{ads}\sigma^2/L^2$. By placing a fixed number of chains on surfaces of various sizes, we simulated surface densities up to that corresponding to the critical overlap concentration. In other words, we approached the semidilute regime within the adsorbed film. During equilibration runs near the critical overlap concentration, some of the polymers were seen to desorb as the system approached the steady state.

We first consider the average bound fraction $\langle \Phi_a \rangle$ and maximum height $\langle h \rangle$, presented in Fig. 5. Results are shown as functions of the surface bead density ρ^* for chains of $N = 50$, 100, and 200 beads with bead-surface interaction parameters $0.4 \leq \varepsilon^*_s \leq 1.0$. For comparison, points for isolated chains are shown at $\rho^* = 0$, the effective density in this case. In all cases, $\langle \Phi_a \rangle$ decreases with

increasing $\rho*$. This may be explained by the entropic penalty associated with a reduced number of molecular conformations due to crowding; this effect becomes more pronounced as the surface density is increased. With purely repulsive bead-bead interactions, there is no additional energetic gain upon adsorption (above the bead-surface interaction) to offset the growing entropic penalty. Hence, it is more favourable for some beads to lift off the surface to ease crowding. Some additional observations are that for a given N and $\rho*$, $\langle \Phi_a \rangle$ increases with increasing ε^*_s; and that for a given $\rho*$ and ε^*_s, $\langle \Phi_a \rangle$ is essentially independent of N. We note that $\langle \Phi_a \rangle$ has been examined in experiments on linear-polymer films,[51] but these were conducted with chemisorbed molecules, as opposed to the physisorbed molecules considered in this work. Chemisorption reduces sorbate mobility, and hence reduces the opportunity for reorganization. In addition, molecules can be irreversibly chemisorbed through fewer surface contacts than those required for physisorption. Both of these effects lead to relatively low bound fractions, as compared to the results reported here.
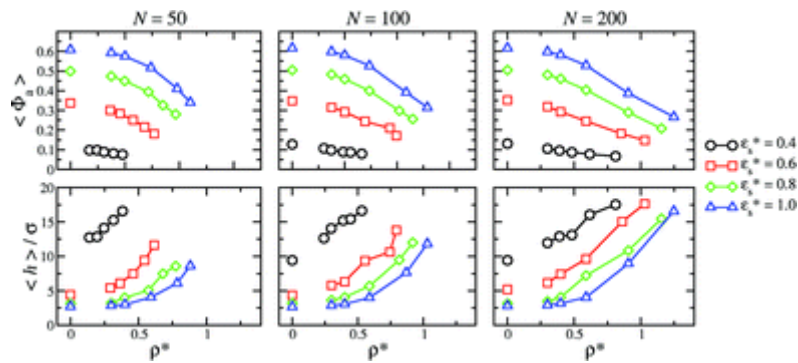

Figure 5. The bound fraction $\langle \Phi_a \rangle$ (top) and the average maximum height $\langle h \rangle$ (bottom) against surface bead density $\rho*$ for many linear chains with, from left to right, $N = 50$, 100, and 200 beads, in good solvent ($\lambda = 0$) and with different surface-interaction parameters ε^*_s. Wherever possible, the corresponding isolated-polymer results are shown at $\rho* = 0$.

Examples of the structural differences between weak and strong surface parameter cases are illustrated in the simulation snapshots shown in Fig. 6. These are from simulations of chains with $N = 100$ beads. With $\varepsilon^*_s = 0.4$ and at $\rho* = 0.39$, the polymers form 'loops' and 'tails', orientated away from the surface; with $\varepsilon^*_s = 1.0$ and at $\rho* = 0.59$, the polymers are flat on the surface, despite the high density.
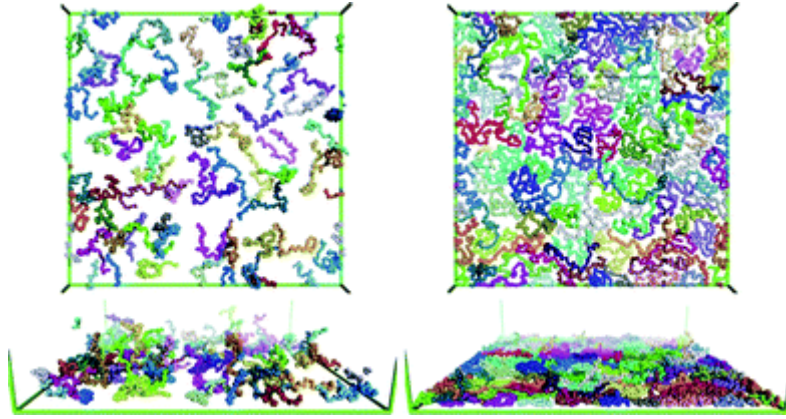
Figure 6. Top views (top) and side views (bottom) from simulations of chains with $N = 100$ beads in good solvent ($\lambda = 0$). The surface dimensions are $130\sigma \times 130\sigma$. (Left) $\varepsilon^*_s = 0.4$, $\rho^* = 0.39$, $N_{ads} = 6600$. (Right) $\varepsilon^*_s = 1.0$, $\rho^* = 0.59$, $N_{ads} = 10\,000$. Figures were prepared using Pymol (http://pymol.sourceforge.net/).

Variations in the average maximum height $\langle h \rangle$, shown in Fig. 5, correlate with those in $\langle \Phi_a \rangle$. As the bound fraction decreases, the film height increases, reflecting the build-up of the polymerfilm. Scaling theory predicts that the height $\langle h \rangle$ scales like $\varepsilon_s^{\nu/(\nu-1)}$ where ν is the characteristic exponent.[27,52,53] For polymers in good solvent, $\nu = 3/5$ and so $\langle h \rangle \sim \varepsilon_s^{-3/2}$. This applies to isolated polymers, and to many polymers when the surface concentration is much greater than the bulk concentration. Since in all cases we have an effective bulk density of zero, the scaling law should be observed. For each system showing significant adsorption under good-solvent conditions, we fitted $\langle h \rangle$ to the function

$$\langle h \rangle = \frac{h_0}{(\varepsilon^*_s)^{3/2}} \qquad (12)$$

and plotted the quantities $\langle h \rangle / h_0$ on a single graph, as shown in Fig. 7. The results should collapse on to the curve $(\varepsilon^*_s)^{-3/2}$; they are indeed broadly consistent with the predicted scaling. Note that the critical surface-energy parameter is expected to be unimportant in this analysis, because we are working in the strong-coupling regime. From the fit shown in Fig. 7, it is clear that the critical value of ε^*_s would be small compared to the values used in the simulations. Indeed, attempts to fit critical parameters led to values of no more than 0.1, in reduced units, but with relative statistical uncertainties approaching 100%.
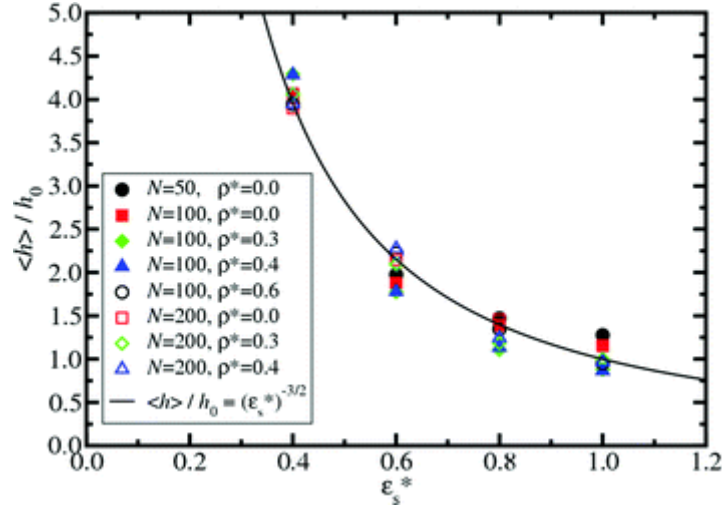
Figure 7. Scaling plot of the maximum height $\langle h \rangle$ against the surface-interaction parameter ε^*_s for polymers in good-solvent conditions ($\lambda = 0$). A reduced density of $\rho^* = 0$ corresponds to isolated polymers . The theoretical prediction[27,52,53] is that $\langle h \rangle \sim \varepsilon_s^{\nu/(\nu-1)}$, which for good-solvent conditions ($\nu = 3/5$) gives $\langle h \rangle \sim \varepsilon_s^{-3/2}$. h_0 is the constant of proportionality from eqn (12).

The effects of the surface-interaction parameter on the conformations of polymers in good-solvent conditions can be characterized in terms of the radius of gyration R_G defined by

$$R_G^2 = \left\langle \frac{1}{N^2} \sum_{i=1}^{N} \sum_{j>i}^{N} \left| r_i - r_j \right|^2 \right\rangle \tag{13}$$

We note that R^2_G can be decomposed into components perpendicular and parallel to a surface, but the average value defined above is sufficient for the current purposes. Fig. 8 shows the ratio γ $=R^2_G(\text{many})/R^2_G(\text{isolated})$, where R^2_G (many) is for many polymers made up of $N = 200$ beads in good-solvent conditions and at finite density, and R^2_G (isolated) is the corresponding value for an isolated polymer on a surface (and therefore at an effective density of $\rho^* = 0$). Results are shown for systems with various surface-interaction parameters. For a given ε^*_s, increasing the density causes a decrease in γ, reflecting a crowding effect due to neighbouring polymers . For a given ρ^*, increasing ε^*_s causes a flattening of the polymers , and hence an overall reduction in the average dimensions.
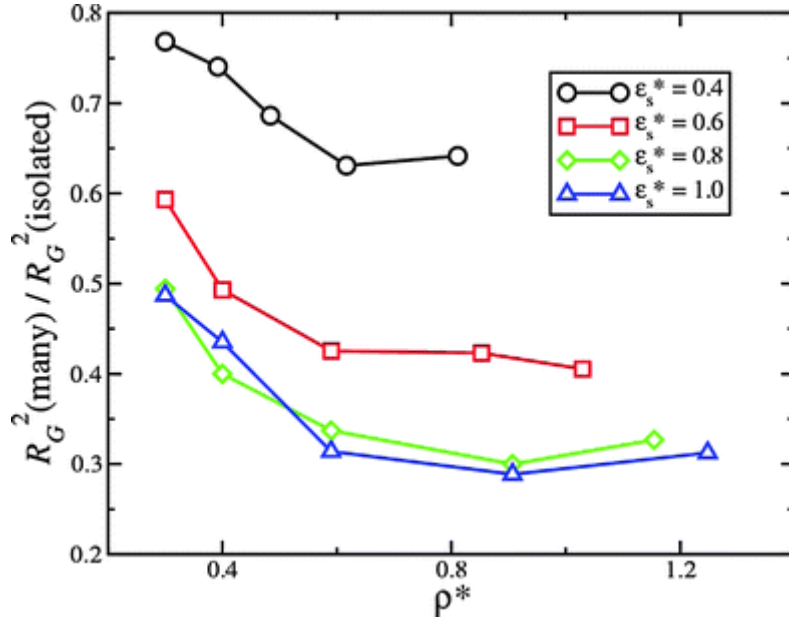
Figure 8. R^2_G for many polymers , divided by R^2_G for an isolated polymer , against surface bead density ρ^*, for polymers with $N = 200$ beads in good-solvent conditions and with various surface-interaction parameters ε^*_s.

The probability density $p(z)$ for the many-polymer case is shown in Fig. 3(c). Specifically, we show results for chains consisting of $N = 100$ beads, with $\lambda = 0$, a fixed surface-interaction parameter $\varepsilon^*_s =$ 1.0, and surface bead densities ranging from $\rho^* = 0$ (isolated chain) to $\rho^* = 1.0$. The proximal regime, identified by de Gennes,[32] is dominated by the bead-surface interactions, and in this case covers the range $0 \leq z/\sigma \leq 2$; the two peaks can be interpreted as arising from two ordered layers on the surface. For an isolated chain, $p(z)$ dies off very rapidly beyond $z \simeq 2\sigma$. At finite densities, $p(z)$ dies off rapidly at large distances, roughly corresponding to the distal regime. Under the same conditions, there is an intermediate, central regime in which $p(z)$ should vary like $z^{-4/3}$ in good-solvent conditions;[27] our simulation results appear to be consistent with this scaling law. For the system with $\rho^* = 1.0$, the central regime covers the range $2 \leq z/\sigma \leq 10$; approximate ranges of the proximal, central and distal regimes for this system are indicated in Fig. 3(c). In general, the theoretical scaling predictions should apply to long chains and to adsorption from semidilute solutions. The experimental[31] and simulation conditions correspond more closely to those of an adsorbed film in contact with a pure solvent ; in addition, the simulated chains are relatively short. Our results approach the expected $z^{-4/3}$ scaling with increasing density, as the conditions *near the surface* begin to resemble those in a film formed by adsorption from semidilute solutions. We note that the upper limit of the apparent central regime ($\sim$ 10σ) is comparable to the radius of gyration of an isolated polymer ($\sim N^\nu$) with $N = 100$ monomers. We emphasize that this study was not focused on observing the predicted scaling, but it is comforting

that our simulation results are at least consistent with the theoretical predictions;[28,29,32] coarse-grained, off-lattice models of polymers in good solvent appear to form de Gennes' 'self-similar carpet'.[29]

C. Many polymers —bad solvent

The final step in the experimental polymer -adsorption procedure being considered here, is the quench from good-solvent to bad-solvent conditions, corresponding to rinsing with solvent and then drying in nitrogen /air. In our simulations, we mimic this step by starting simulations from well equilibrated configurations with $\lambda = 0$ (good solvent) and then instantaneously switching to $\lambda = 1$ (bad solvent). We then re-equilibrate the system for $2 \times 10^6 \delta t$, during which time the system was seen to reach an apparent steady state. In our experiments, the surfaces were imaged after having been stored at room temperature (~ 125 K above the glass-transition temperature) for periods of several weeks; the observed cluster structures may well represent the equilibrium, or close-to-equilibrium, state, since the system has had time and sufficient thermal energy to relax. In our simulations no restrictions exist in the lateral directions, *e.g.*, surface roughness, thus allowing the polymers slowly to diffuse on the surface. In earlier simulations of polymer films on surfaces, apparently metastable structures have been observed for periods of time that might extend towards experimental timescales.[54] Simulations therefore provide valuable insights on the experimental images. Nevertheless, it is easy to imagine that the true equilibrium state—if accessible—would correspond to a single, large (hemispherical)polymer droplet;[17–19] so the observed behaviour in our simulations might best be described as metastable. This is because the diffusion rate of an absorbed polymer chain in a bad solvent is not only lower than that in a good solvent , but also inversely proportional to the number of beads.[20] Thus, within the simulation timescale, clusters and isolated chains may not diffuse sufficiently far in order to form a putative, single-droplet equilibrium structure. In any case, the structures we observe are apparently static on the timescales accessed in the simulations.

Fig. 9 shows examples of equilibrated simulation configurations before ($\lambda = 0$) and after ($\lambda = 1$) the quench, for systems of polymers each made up from $N = 200$ beads, with surface-interaction parameters $\varepsilon^*_s = 0.4$, and at various densities. In good-solvent conditions, the polymers are in extended conformations, but in bad-solvent conditions they collapse to form globular clusters to optimize the attractive bead-bead interactions. At high density ($\rho^* = 0.81$) the quench induces extensive clustering, resulting in a small number of large clusters . At intermediate density ($\rho^* = 0.49$), a mixture of single chains and large clusters is in evidence, with the single chains in the minority. At low density ($\rho^* = 0.30$) the single chains are more numerous.
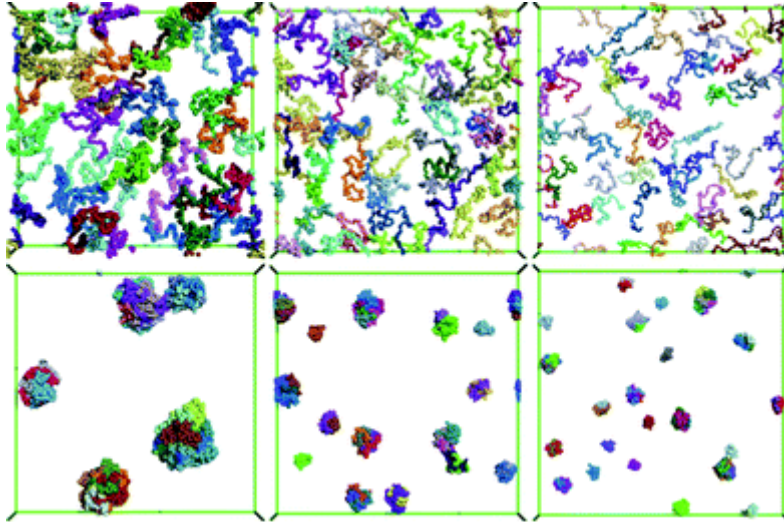
Figure 9. Top views from simulations of chains with $N = 200$ beads in good-solvent conditions ($\lambda = 0$, top) and bad-solvent conditions ($\lambda = 1$, bottom), and with surface-interaction parameter $\varepsilon^*_s = 0.4$. (Left) $\rho^* = 0.81$, $L = 80\sigma$, $N_{ads} = 5200$. (Center) $\rho^* = 0.49$, $L = 130\sigma$, $N_{ads} = 8200$. (Right) $\rho^* = 0.30$, $L = 180\sigma$, $N_{ads} = 9720$. Figures were prepared using Pymol (http://pymol.sourceforge.net/).

In Fig. 10 we show cluster -size histograms for systems of polymers ($N = 200$ beads per polymer) in bad-solvent conditions, with fixed surface bead density $\rho^* = 0.30$, and with various surface-interaction parameters ε^*_s. Two polymers were considered clustered if any two beads on different polymers were within a distance of 1.5σ. Histograms were accumulated from sets of five independent good solvent-to-bad solvent simulations. With small surface-interaction parameters ($\varepsilon^*_s = 0.4$ and 0.6) the distribution shows a monotonic decrease from the peak corresponding to single chains; with larger parameters ($\varepsilon^*_s = 0.8$ and 1.0), the distribution is bimodal, with a clear delineation between one-chain and two-chain species, and larger clusters . The bimodal distribution is to be compared qualitatively to that found in AFM experiments, Fig. 1(b). A direct, quantitative comparison is not feasible because we have not considered a specific, coarse-grained molecular model tailored to describe 78.8 kg mol^{-1} linear PB adsorbed on mica. Another factor that might influence the pattern formation, and that has not been considered in the simulations, is polydispersity in the lengths of the chains. Nonetheless, we suggest that the general picture, to be sketched out below, will apply to the real, experimental situation.
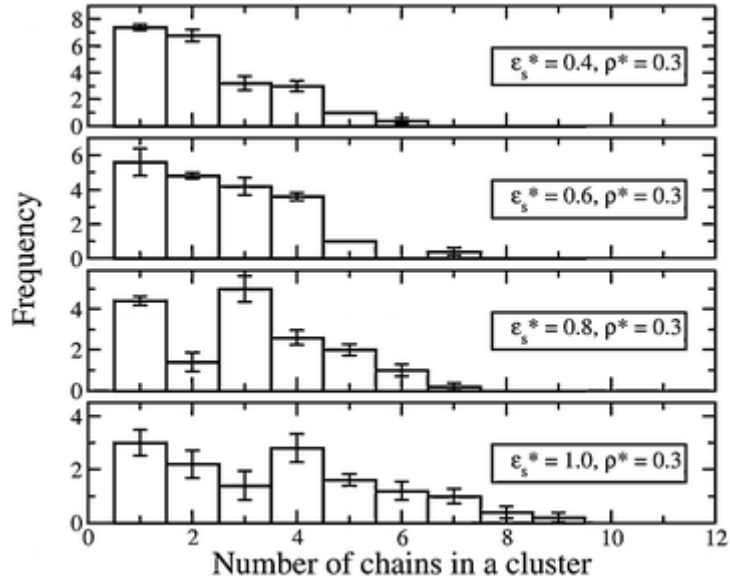
Figure 10. Cluster -size histograms from simulations of polymers with $N = 200$ beads in bad-solvent conditions ($\lambda = 1$), at a density $\rho^* = 0.30$, and with various surface-interaction parameters. Each histogram is an average of five independent simulations of the good-solvent to bad-solvent quenching process. In each case, the total number of adsorbed beads (as defined in section IIIB) is $N_{ads} = 10\,000$.

Clearly, the nature of the cluster -size distribution depends on both ρ^* and ε^*_s. From simulations of 200-bead polymers at different densities and with different surface-interaction parameters, we constructed a 'phase diagram' indicating whether the quenched configurations in bad-solvent conditions showed monotonically decreasing cluster -size distributions, bimodal distributions, or distributions showing single peaks; it is shown in Fig. 11. In general, low ρ^*/low ε^*_s favours a monotonically decreasing cluster distribution. Increasing ε^*_s flattens out the polymers on the surface, while increasing ρ^* slightly leads to more overlaps with neighbouring chains; either change leads to more pronounced clustering and a bimodal cluster distribution. At high values of ρ^* and ε^*_s, the clustering is extensive and the cluster -size distribution is strongly peaked (typically at around five chains per cluster).
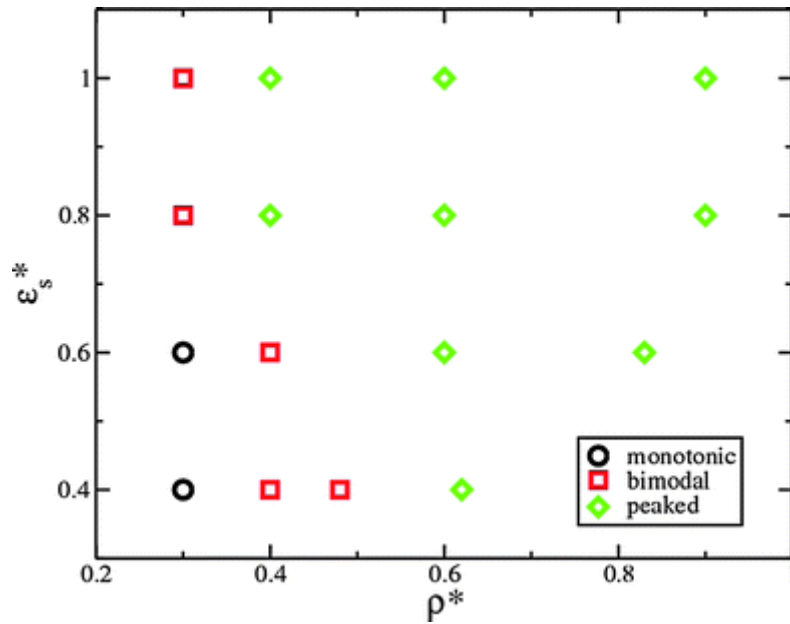
Figure 11. 'Phase diagram' in the plane of surface density ρ^* and surface-interaction parameter ε^*_s for polymers with $N = 200$ beads in bad-solvent conditions ($\lambda = 1$), showing the occurrences of cluster distributions which are either monotonic decreasing with cluster-size, bimodal, or single peaked.

From these results, we can picture the polymer behaviour during the good solvent-to-bad solvent quench as follows. At low density and with a low surface-interaction parameter, the polymers are largely isolated from one another and the probability of forming bead-bead contacts is low because of the large mean separation and the existence of 'loops' and 'tails' extending perpendicular to the surface. The polymer conformations are essentially the same as for an isolated polymer . During the quench, the majority of polymers simply fold up by themselves; successively smaller proportions of the molecules form dimers, trimers, etc., leading to a monotonic, rapidly decaying cluster distribution. At high density and with a high surface-interaction parameter, the polymers are held flat on the surface and hence the chains form many more contacts with their neighbours. Therefore, during the quench, polymers aggregate with their neighbours and go on to form large clusters . The cluster distribution is consequently peaked at a relatively large value. At intermediate values of the density or the surface-interaction parameter, the polymer conformations are not significantly different from those of isolated polymers , but there are many more opportunities for forming contacts with neighbours. These factors favour a mixture of the extremal processes described above, and so give rise to a bimodal cluster distribution.

4. Conclusions

In this work we have used Langevin dynamics simulations of a coarse-grained, bead-spring model to gain insight on the adsorption of linear polymers on to a smooth surface. The main experimental results we set out to understand are AFM images of polymers physisorbed from solution on to mica surfaces during a process of rapid solvent evaporation . We mimicked this process by switching the bead-spring model interactions from good-solvent to bad-solvent conditions. Of particular interest was the experimental observation of a bimodal cluster distribution. We have shown that this feature is favoured at low-to-moderate polymer concentrations, and over a broad range of polymer -surface interaction strengths. At high concentrations, a single-peaked distribution is observed; at low concentrations, and with weak polymer -surface interactions, a monotonically decaying cluster distribution is obtained. The trends observed in simulations have been rationalized in terms of the probable numbers of contacts between polymers before quenching from good-solvent to bad-solvent conditions.

We have measured and rationalized the trends in a variety of other properties including the fraction of monomer units bound to the surface, the height of the adsorbed polymer film, and the radius of gyration of an adsorbed polymer chain. An additional, incidental result of this study is the reproduction of an algebraically decaying density profile within the 'central regime', as predicted by de Gennes using scaling arguments;[32] the simulation results are consistent with the prediction that the monomer density as a function of the perpendicular distance from the surface (z) decays like $z^{-4/3}$. The existence of the central regime has been confirmed experimentally[33–36] and in Monte Carlo simulations of lattice models,[37–39] but as far as we are aware, this has not been demonstrated before in simulations of an off-lattice model.

Future simulation work will be focused on the adsorption and clustering of star polymers on smooth surfaces. In addition, the kinetics of adsorption and clustering will be explored in detail. For now, we note that two distinct mechanisms for the self-assembly of adsorbed polymers were identified through inspecting movies of the simulated quenching process. In the first mechanism, weakly adsorbed chains first collapse into individual globules, which then slowly diffuse over the surface and coalesce. The cluster distribution then apparently reaches a steady state on the simulation timescale. This process was more common with small chains (with $N = 50$ beads) at low concentrations. The second mechanism involves the development of contacts between the polymers prior to quenching, *i.e.*, in good-solvent conditions. Upon quenching, the chains collapse into one another, and form more extended structures. Occasionally, we observed a chain bridging between two others, and causing all three to collapse simultaneously. These mechanisms were favoured by longer chains ($N = 200$ beads) at high concentrations. A detailed simulation study of the kinetics of the adsorption and clustering processes is in progress.

References

[1] D. H. Napper, *Polymeric Stabilization of Colloidal Dispersions*, Academic Press, London, 1983.

[2] A. P. Gast and L. Leibler, *Macromolecules*, 1986, **19**, 686–691.

[3] J. K. Cox, A. Eisenberg and R. B. Lennox, *Curr. Opin. Colloid Interface Sci.*, 1999, **4**, 52–59.

[4] K. B. Migler, H. Hervet and L. Leger, *Phys. Rev. Lett.*, 1993, **70**, 287–290.

[5] H. R. Brown, *Science*, 1994, **263**, 1411–1413.

[6] P. O. Brown and D. Botstein, *Nature Genetics Supplement*, 1999, **21**, 33–37.

[7] E. Pludeman and N. Collins, *Adhesion Science and Technology*, Vol. 9a, Plenum Press, New York, 1975.

[8] R. Viswanathan, J. Tian and D. W. M. Marr, *Langmuir*, 1997, **13**, 1840–1843.

[9] G. Bar, Y. Thomann and M.-H. Whangbo, *Langmuir*, 1998, **14**, 1219–1226.

[10]   D. Raghavan, X. Gu, T. Nguyen, M. Van Landingham and A. Karim, *Macromolecules*, 2000, **33**, 2573–2583.

[11]   J. C. Meiners, A. Quintel-Ritzi, J. Mlynek, H. Elbs and G. Krausch, *Macromolecules*, 1997, **30**, 4945–4951.

[12]   J. Kumaki and T. Hashimoto, *J. Am. Chem. Soc.*, 2003, **125**, 4907–4917.

[13]   J. C. Zhao, S. Z. Tian, Q. Wang, X. B. Liu, S. C. Jiang, X. L. Ji, L. An and B. Z. Jiang, *Eur. Phys. J. E*, 2005, **16**, 49–56.

[14]   V. Koutsos, E. W. van der Vegte, E. Pelletier, A. Stamouli and G. Hadziioannou, *Macromolecules*, 1997, **30**, 4719–4726.

[15]   V. Koutsos, E. W. van der Vegte and G. Hadziioannou, *Macromolecules*, 1999, **32**, 1233–1236.

[16]   K. Furukawa, *Acc. Chem. Res.*, 2003, **36**, 102–110.

[17]   A. Milchev and K. Binder, *Macromolecules*, 1996, **29**, 343–354.

[18]   K. Binder, A. Milchev and J. Baschnagel, *Annual Reviews Mater. Sci.*, 1996, **26**, 107–134.

[19]   A. Milchev and K. Binder, *J. Chem. Phys.*, 2001, **114**, 8610–8618.

[20]   D. Mukherji, G. Bartels and M. H. Müser, *Phys. Rev. Lett.*, 2008, **100**, 068301.

[21]   Y. Wang and R. Rajagopalan, *J. Chem. Phys.*, 1996, **105**, 696–705.

[22]   H. X. Guo, X. Z. Yang and T. Li, *Phys. Rev. E*, 2000, **61**, 4185–4193.

[23]   N. Källrot and P. Linse, *Macromolecules*, 2007, **40**, 4669–4679.

[24]   J. Luettmer-Strathmann, F. Rampf, W. Paul and K. Binder, *J. Chem. Phys.*, 2008, **128**, 064903.

[25]   R. Descas, J.-U. Sommer and A. Blumen, *J. Chem. Phys.*, 2006, **125**, 214702.

[26]   S. Metzger, M. Müller, K. Binder and J. Baschnagel, *J. Chem. Phys.*, 2003, **118**, 8489–8499.

[27]   P. G. de Gennes, *Scaling Concepts in Polymer Physics*, Cornell University Press, Cornell, 1st edn, 1979.

[28]   E. Bouchaud and M. Daoud, *J. Phys.*, 1987, **48**, 1991–2000.

[29]   A. N. Semenov, J. Bonet-Avalos, A. Johner and J. F. Joanny, *Macromolecules*, 1996, **29**, 2179–2196.

[30]   E. Glynos, A. Chremos, G. Petekidis, P. J. Camp and V. Koutsos, *Macromolecules*, 2007, **40**, 6947–6958.

[31]   E. Glynos, A. Chremos, G. Petekidis, P. J. Camp, E. Theofanidou, and V. Koutsos, to be published.

[32]   P. G. de Gennes, *Macromolecules*, 1981, **14**, 1637–1644.

[33]   L. Auvray and J. P. Cotton, *Macromolecules*, 1987, **20**, 202–207.

[34]   L. T. Lee, O. Guiselin, B. Farnoux and A. Lapp, *Macromolecules*, 1991, **24**, 2518–2522.

[35]   O. Guiselin, L. T. Lee, B. Farnoux and A. Lapp, *J. Chem. Phys.*, 1991, **95**, 4632–4640.

[36]   O. Guiselin, *Europhys. Lett.*, 1992, **17**, 225–230.

[37]   J. de Joannis, R. K. Ballamudi, C.-W. Park, J. Thomatos and I. A. Bitsanis, *Europhys. Lett.*, 2001, **56**, 200–206.

[38]   J. de Joannis, C.-W. Park, J. Thomatos and I. A. Bitsanis, *Langmuir*, 2001, **17**, 69–77.

[39]   P. Cifra, *Macromol. Theory Simul.*, 2003, **12**, 270–275.

[40]   T. A. Witten and P. A. Pincus, *Structured fluids: polymers, colloids, surfactants*, Oxford University Press, Oxford, 2004.

[41]   S. O. Nielsen, C. F. Lopez, G. Srinivas and M. L. Klein, *J. Phys.: Condens. Matter*, 2004, **16**, R481–R512.

[42]   G. S. Grest and K. Kremer, *Phys. Rev. A*, 1986, **33**, 3628–3631.

[43]   G. S. Grest, K. Kremer and T. A. Witten, *Macromolecules*, 1987, **20**, 1376–1383.

[44]   G. S. Grest, *Macromolecules*, 1994, **27**, 3493–3500.

[45]   S. W. Sides, G. S. Grest and M. J. Stevens, *Macromolecules*, 2002, **35**, 566–573.

[46]   M. O. Steinhauser, *J. Chem. Phys.*, 2005, **122**, 094901.

[47]   J. D. Weeks, D. Chandler and H. C. Andersen, *J. Chem. Phys.*, 1971, **54**, 5237–5247.

[48]   M. P. Allen and D. J. Tildesley, *Computer Simulation of Liquids*, Clarendon Press, Oxford, 1987.

[49]   E. Eisenriegler, *Polymers Near Surfaces*, World Scientific, River Edge, 1993.

[50]   E. Eisenriegler, K. Kremer and K. Binder, *J. Chem. Phys.*, 1982, **77**, 6296–6320.

[51]   P. Frantz and S. Granick, *Macromolecules*, 1995, **28**, 6915–6925.

[52]   M. Rubinstein and R. H. Colby, *Polymer Physics*, Oxford University Press, Oxford, 2003.

[53]   R. R. Netz and D. Andelman, *Phys. Rep.*, 2003, **380**, 1–95.

[54]   D. Mukherji and M. H. Müser, *Macromolecules*, 2007, **40**, 1754–1762.